International Journal of ChemTech Research
CODEN (USA): IJCRGG ISSN: 0974-4290
Vol.8, No.4, pp 1923-1934, 2015

Growth and Characterization of Lithium Sulphate Monohydrate Single crystal

S. Bagavathi[1], D. Muthuraj[2], P. Selvarajan[3]*, D. Shanthi[3]

[1]Department of Physics , National Engineering College, Kovilpatti, India
[2]Department of Physics , M.D.T Hindu College, Tirunelveli, India
[3]Department of Physics , Aditanar College of Arts and Science, Tiruchendur, India

Abstract: A new potentially useful nonlinear optical (NLO) inorganic material, Lithium Sulphate Monohydrate (LSM) has been synthesized and grown as a high-quality single crystal by the slow evaporation technique. The grown crystals were characterized by Fourier transform infrared spectroscopic (FTIR) analysis to find the different modes of vibration due to various functional groups present in the crystal. The powder X-ray diffraction pattern of the grown crystal has been studied and the sharp peaks observed in powder X-ray diffraction studies confirm the high degree of crystallinity of grown crystal. The optical transmission spectrum was investigated to study its linear optical properties using UV–vis-NIR spectrophotometer. The thermal behaviour of LSM has been analyzed using TG/DTA thermal curves. From the thermal study, the material is found to possess the thermal stability up to 156 ^{o}C. The mechanical property of the grown crystal has been studied using Vicker's micro hardness tester. The microstructure of the grown crystal and the presence of various elements in the crystal were analyzed using SEM and EDAX techniques. The nonlinear optical property was tested using Kurtz Perry powder technique and SHG efficiency was measured.

1. Introduction

For the past three decades, the field of electronics, fibre optic communication and lasers has experienced tremendous advancements. Recently, the non-linear optical (NLO) materials are gaining keen attention due to their enormous applications in emerging optoelectronic technologies. The growth of high-quality single crystals remains a challenging endeavor for material science. Crystals of a large size with structural perfection are required for fundamental research and practical implementation in photonic and optoelectronic technology. Inorganic NLO materials exhibit excellent mechanical and thermal properties. Sulphates are of great interest in industry, due to their outstanding physical properties and widely used as nonlinear optical (NLO), ceramic, ferroelectric, electric, and catalytic materials [1–8]. Especially, a great deal of interest has focused on the exploration of NLO materials for the development of frequency doubling crystal. For example, KH_2PO_4 (KDP) is among the most widely-used commercial NLO material, and it is commonly used for doubling, tripling and quadrupling of Nd: YAG laser at the room temperature [9–11]. The design of optoelectronics and photonic devices realizes heavily in the development of nonlinear optical materials with higher efficiency. So the materials possessing large second order nonlinear susceptibility with favorable in thermal and mechanical stability are intensively used in many device applications [12–14]. Lithium Sulphate Monohydrate (LSM) crystals have been crystallized and studied in the present work. Lithium Sulphate Monohydrate crystallizes in $P2_1$ space group with monoclinic structure. Crystal growth, characterization and SHG studies were already made recently [15]. The results of the growth, the powder X-ray diffraction studies, FTIR studies, UV-vis-NIR studies, TGA-DTA, microhardness, SEM analysis with EDAX and SHG studies of the grown crystals are reported in this paper.

2. Experimental procedure

2.1. Synthesis and growth of LSM

The starting material LSM ($Li_2SO_4.H_2O$) was taken and 20 g of material was dissolved in 70 ml de-mineralised water at room temperature of 32 ^oC. The solution was continuously stirred with a magnetic stirrer for about 4 hours to attain homogeneity and the solution was allowed to undergo slow evaporation which gradually led to supersaturated condition for the nucleation of crystal phase resulting in the formation of tiny crystals. The crystallization process was repeated three times to improve the size and quality of the crystal as it is essential before proceeding further. After a period of 32 days, good quality transparent single crystals of LSM with dimensions of 2.2 cm×1.9 cm×0.6 cm were harvested successfully. The photograph of the grown crystal is shown in **Fig.1.**

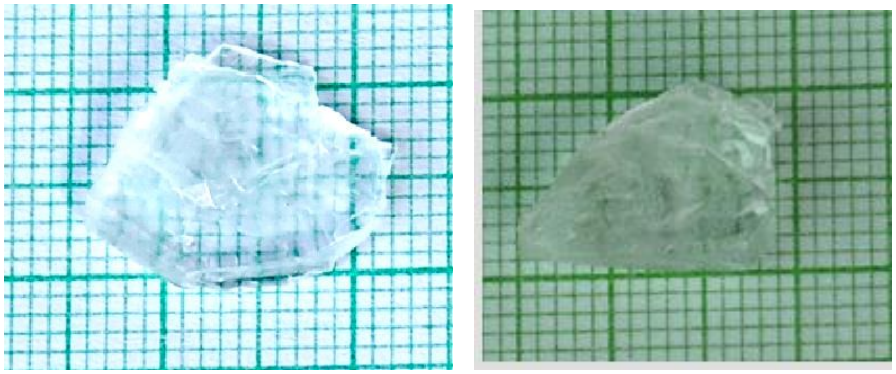

Fig.1. Photograph of grown LSM crystals

2.2. Solubility Studies and induction period measurement

The size and growth rate of a crystal depends on the solubility and temperature of the solution. The solubility of Lithium Sulphate Monohydrate was determined by gravimetrical method [16] at different temperatures. The $Li_2SO_4.H_2O$ has negative solubility behaviour .The solubility of the material is reverse, i.e. with increasing temperature the solubility decreases. The solubility of LSM in water was determined as a function of temperature in the range 25 ^oC - 45 ^oC in steps of 5 ^oC. The salt was added to 100 ml de-mineralised water for the measurement of solubility. Initially, the solution was maintained at a constant temperature of 25 ^oC and continuously stirred using a hot plate magnetic stirrer for about 3 hours and a digital thermometer was used to ensure homogeneous temperature. The temperature of the solution can be maintained with an accuracy of 0.1 ^oC. The homogeneous concentration was also maintained throughout the volume of the solution. After attaining the saturation, the solubility was determined gravimetrically. The same procedure was followed for other temperatures. The temperature of the solution was controlled using the voltage regulator attached with the magnetic stirrer. At 25 ^oC 40.8 g of the compound was dissolved and at 45 ^oC 37 g was dissolved. The solubility curve of LSM is shown in **Fig. 2.**

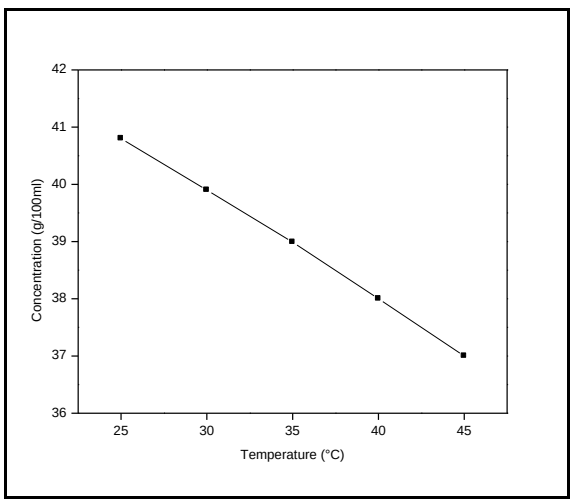

Fig.2. Solubility curve of LSM sample

For the measurement of induction period, isothermal method [17] was used at the selected supersaturation ratio (S) 1.05 at the temperature of 45 ^{o}C. Using the solubility diagram, the synthesized salt of LSM was used to prepare supersaturated aqueous solution (by keeping S at 1.05) in a corning glass beaker (nucleation cell) and it was stirred continuously for about 2 hours using a magnetic stirrer to ensure the homogeneous concentration. The prepared solution was cooled 10 ^{o}C below saturation temperature for homogenization and it was taken to the desired temperature. When the desired temperature and concentration were reached, the solution was maintained at that temperature and the nucleation cell was loaded in a constant temperature bath and illuminated using a powerful lamp to observe the formation of nucleus and a stop clock was put on. When the first speck of nucleation occurred in the solution, the time was noted. This time of observation of the first speck particle in the nucleation cell from the time at which the solution reached the experimental temperature was the induction period (τ).The induction period observed is 589 seconds. It is concluded from the experiment that the crystal should be grown well within the critical supersaturation in order to obtain good quality crystals for device fabrications.

2.3. Instrumentation

A grown LSM crystal was subjected to powder X-ray diffraction pattern using XPERT PRO diffractometer using Cu K_{α} radiation (with λ = 1.5406 Å at 35 kV, 10 mA) to identify the reflection planes. The sample was scanned over the required range for 2θ values (10^{o}–80^{o}) in steps of 0.05^{o}. The crystalline phase of the sample was identified from the crystallographic parameters such as 2θ and hkl values. The infrared spectroscopy is effectively used to identify the functional groups of the grown crystals and the FTIR spectrum of the sample was recorded using Thermo Nexus 670 spectrometer with MCT-B Detector in the range 400–4000 cm^{-1}. Simultaneous thermo gravimetric (TG) and differential thermal analysis (DTA) were carried out for LSM sample using a STD Q600 V8.3 Build 101 thermal analyzer in nitrogen atmosphere for the temperature range 40 ^{o}C – 750 ^{o}C at a heating rate of 20 ^{o}C min^{-1}. The optical transmission spectrum of LSM crystal has been recorded in the region 190–800 nm using a UV–vis-NIR spectrometer of Arithmetic Model with Scan speed of 480 nm/min and Data interval of 1nm. For this study, an optically polished single crystal of thickness 4 mm was used. Mechanical property was studied by measuring micro hardness of the grown crystal and this was carried out using Vicker's micro hardness tester of Shimadzu Model HMV 2T fitted with a diamond indenter. Smooth, flat surface of the grown LSM crystal was selected and subjected to this study. Indentations were made for various loads from 25 g to 100 g. The microstructure of the grown crystal and the presence of various elements in the crystal were analyzed using SEM and EDAX techniques using JEOL-JSM 5300 scanning electron microscope with a magnification of 30 k. SHG efficiency of the grown crystal was measured by Kurtz and Perry Powder technique. The fundamental beam of 1064 nm from Q-switched Nd:YAG laser was used to test the SHG property of the grown crystal. The input pulse with energy 3.5 mJ/pulse and pulse width of 10 ns with a repetition rate of 10 Hz was used. The fundamental beam was filtered by using IR filter. A photo multiplier tube (Philips photonics) was used as detector of the optical output signal emitted by the sample.

3. Results and discussion

3.1. Powder XRD analysis

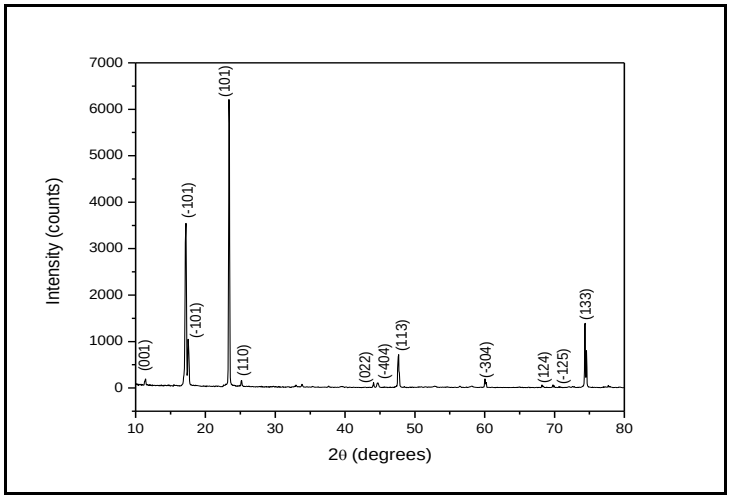

The grown crystals of pure LSM were crushed into fine powder and powder X-ray diffraction analysis has been carried out using X-ray diffractometer. The sample was subjected to intense X-ray at a scan speed of 1 ^{o}/min to obtain lattice parameters. The recorded patterns are shown in **Fig. 3** .The sharp peaks of XRD pattern indicate high degree of crystalline structure of grown LSM crystal. The observed diffraction pattern has been indexed and Miller indices were estimated by index software package. X-ray pattern of LSM was used to calculate lattice parameters using unit cell. It is found that there is a close agreement with values obtained by single crystal X-ray diffraction. The observed 2θ, d and calculated hkl indices of the corresponding reflecting planes are shown in **Table 1**.

Table 1: X-ray powder diffraction data of LSM crystal.

2θ (°)	d spacing (Å)	hkl
11.375	7.77267	001
17.545	5.05064	$\bar{1}01$
23.371	3.80306	101
25.143	3.53899	110
44.031	2.05493	022
44.634	2.02853	$\bar{1}04$
47.600	1.90881	113
60.041	1.53965	$\bar{3}04$
68.206	1.37387	124
69.763	1.34695	$\bar{1}25$
74.353	1.27475	133

3.2. FTIR Spectrum analysis

FTIR spectroscopic studies were effectively used to identify the functional groups present in the synthesized compound. To analyze qualitatively the presence of the functional groups in LSM crystals, FTIR spectra were recorded using spectrometer in the range 400 - 4000 cm^{-1}. The recorded FTIR spectrum of LSM crystal is shown in **Fig. 4. Table 2** shows the vibrational assignments for LSM crystals.

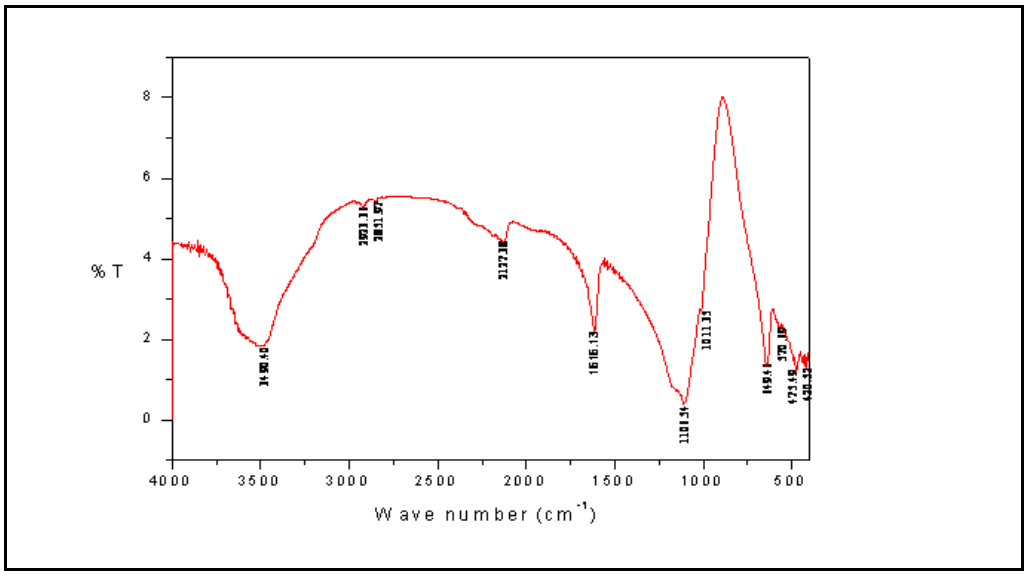

Fig.4. FTIR Spectrum of LSM crystal

The stretching vibrations of the water molecule are expected in 3000-3700 cm^{-1}. The broad vibrational band observed around 3490.40cm^{-1}, is attributed to symmetric stretching mode of water molecule. The medium broad band noticed around 1616.13 cm^{-1} is assigned to the bending vibration of water molecules. In general free SO_4^{2-} ion has 4 fundamental vibrations. The peak at 1555.93 cm^{-1} is assigned to non degenerate stretching mode (ν_1) of SO_4^{2-} ion .The peaks at 1106.54 and 1011.35 cm^{-1} are attributed to SO_4 stretching mode (ν_3). A doubly

degenerated mode (ν_2) and a triply degenerated vibrational mode (ν_4) are at 475.13 $cm^{-1}$and 649.46 cm^{-1} respectively. The mode at 420.07 cm^{-1} is assigned to the vibrational mode δ (Li-O).The above assignment agrees with that already reported. [18-19].

Table 2: Functional group assignment of LSM crystal

Wave number in cm^{-1}	Assignments
3490.40	Symmetric stretching mode of the water molecule
1616.13	Bending vibration of water molecules
1555.93	Stretching (ν_1) of S=O
1106.54	Stretching (ν_3) of SO_4
1011.35	Stretching (ν_3) of SO_4
649.46	Triply degenerate vibrations (ν_4) of SO_4
475.13	Doubly degenerate (ν_2) of SO_4^{2-} mode
420.07	Vibrational mode δ (Li-O)

3.3. Thermal analysis

Thermo gravimetric analysis (TGA) and differential thermal analysis (DTA) of crystal were carried out simultaneously using thermal analyser .A powder sample was used for this analysis in the temperature range of 40 ^{0}C-750 ^{0}C in nitrogen atmosphere at a heating rate of 20 C/min. Thermo gravimetric analysis (TGA) is a technique in which the weight of a substance is recorded as a function of temperature. The derivative or differential thermal analysis (DTA) is the first derivative of the thermo gravimetric curve, which is plotted with respect to either temperature or time. In the present case, the TGA and DTA are carried out between 40.00 ^{o}C to 750.00 ^{o}C at 20 ^{o}C/min in the nitrogen atmosphere which provide an inert environment. The weight, particle size and the mode of preparation (the pre-history) of a sample, all govern the thermo gravimetric results. In practice, a small sample weight is desirable for thermo gravimetric analysis and hence the weight of the sample taken for investigation is 13.159 mg. Both of the thermo grams (TGA and DTA) are recorded in the same chart (**Fig. 5.**). It is seen that loss of water molecule is observed at 156.35 ^{o}C. The range of decomposition 950 ^{o}C – 745 ^{o}C is also confirmed by the prominent endothermic peaks of DTA curve at 138.5 ^{o}C and 578.47 ^{o}C The residue in terms of percentage after the water molecule is released is calculated as 85.99. This value matches well with the observed value of 86. The weight loss thereafter is only about 3% even at an increase of temperature up to 745.6 ^{o}C. Hence, it is inferred that the thermal stability of the title compound is very high.

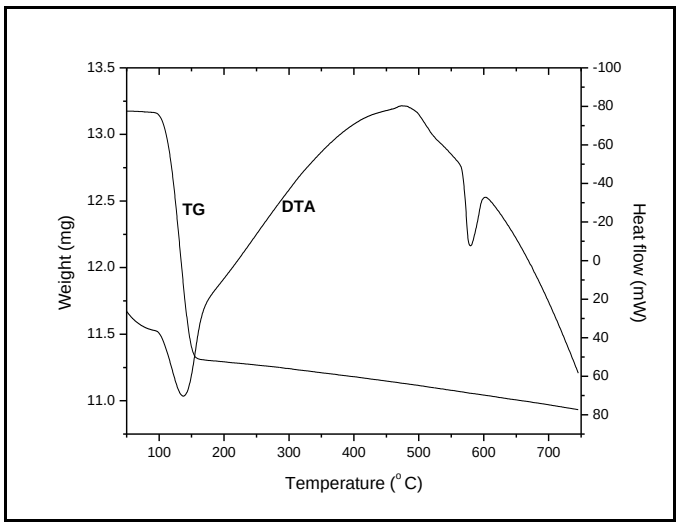

Fig. 5. TG/DTA thermograms for LSM crystal.

3.4. Mechanical analysis

Hardness of the material is a measure of resistance it offers to the local deformation [20]. The structure and composition of the crystalline solids are inviolably related to the mechanical hardness. Micro hardness testing is one of the best methods of understanding the mechanical properties of the materials such as fracture behavior, yield strength, brittleness index and temperature of cracking [21,22]. The hardness of the crystal carries information about molecular binding and elastic constants of the material. Measurement of hardness is a useful non-destructive testing method which is used to determine the applicability of the crystal in the device fabrication. The grown crystals of thickness 4 mm were well polished and placed on the platform of Vickers micro hardness tester. Indentations were made on (1 0 0) face of the crystal and the micro hardness measurements were made for the applied loads varying from 20 to 100 g for the dwell time 5 s. Vickers micro hardness values have been calculated by using the formula Hv = $\frac{1.8544\times P}{d^2}$ kg/mm^2, where H_v is the Vickers micro hardness number, P is the applied load in gram and d is the average diagonal length in mm of the indentation mark.

Fig. 6. shows the variation of H_v as a function of applied load ranging from 20 g to 100 g for the LSM single crystals. It is very clear from the figure that H_v increases with increase in load. The Mayer's index number was calculated from the Mayer's law [23], which relates the load and indentation diagonal length as

$$P = kd^n$$

$$\log P = \log k + n \log d, \qquad (1)$$

where k is the material constant and 'n' is the Meyer's index. In order to find the value of 'n', a graph is plotted for log P against log d (**Fig. 7**.) which gives a straight line (after least square fitting). From the slope line the Meyer's index number 'n' was calculated to be 2.788. According to Onitsch and Hanneman [24] the values of 'n' come out to be 1–1.6 for hard materials and more than 1.6 for soft ones. Thus LSM belongs to soft material category. The above relation indicates that H_v should increase with P if n > 2.This is well satisfied shown by **Fig. 6.** The resistance pressure is defined as a minimum level of indentation load (W) below which no plastic deformation occurs [25]. Hays and Kendall [26] proposed a relationship between indentation test load and indentation size to calculate W by the equation:

$$W = k_1 d^n - k_2 d^2$$

(or)

$$d^n = \left(\frac{W}{k1}\right) + \left(\frac{k2}{k1}\right) d^2 \qquad (2)$$

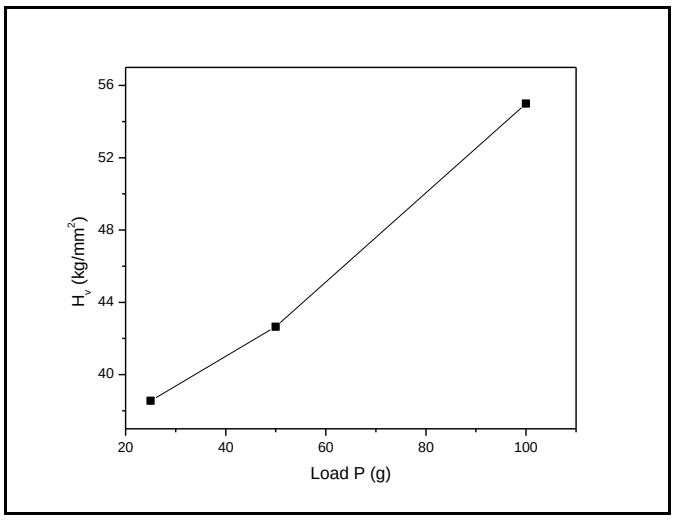

Fig. 6. Variation of Vickers microhardness number H_v with load of LSM crystal

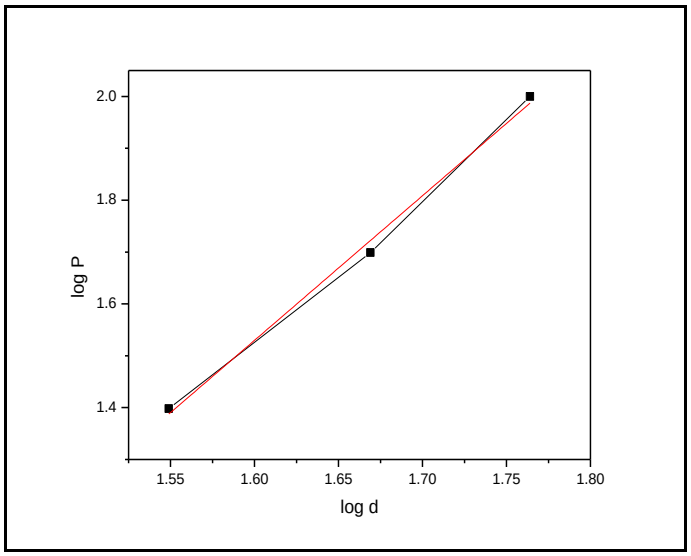

Fig. 7. Graph between log P verses log d of LSM crystal

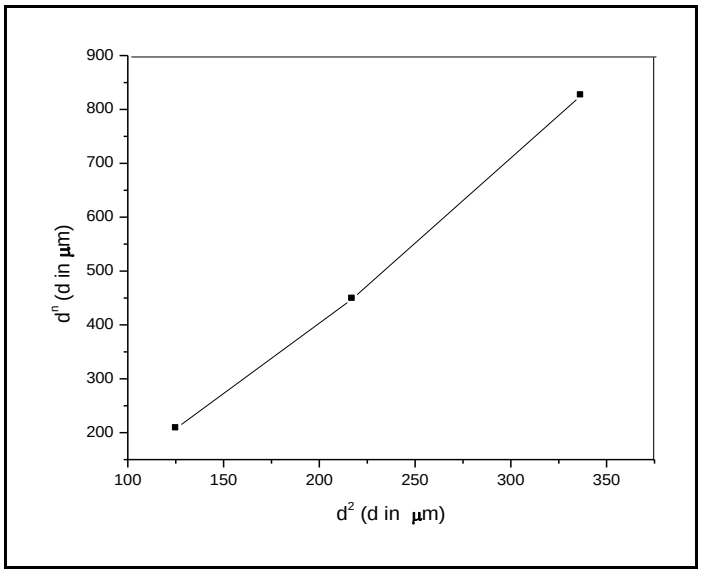

Fig. 8. Graph between d^2 verses d^n of LSM crystal

The plot of d^n vs. d^2 is a straight line (**Fig. 8**.) having slope k2/k1 and intercept W/k1. From these values, we have calculated the value of W (minimum level of indentation load) as 4.98 g.

From Wooster's empirical relation [27],

$$c_{11} = H_v^{7/4}. \qquad (3)$$

The elastic stiffness constant (C_{11}) was calculated by Wooster's empirical relation.

The calculated stiffness constant for different loads was tabulated in **Table 3**.The table shows that the elastic stiffness constant increases with the increase of load. This indicates that the binding force between the ions is strong.

Table.3 Values of elastic stiffness constant for LSM crystal at different loads.

Sl.No.	Load (g)	$C_{11}(\times 10^{14}$ pascal)
1	30	6.16
2	40	6.62
3	50	7.08
4	60	7.85

3.5. Transmittance UV–vis–NIR analysis

The UV–vis transmittance spectrum was recorded for the grown $LiSO_4.H_2O$ crystal using a UV–vis-NIR spectrometer in the range 190–800 nm**. Fig. 9** shows the transmittance spectrum of the LSM crystal. The crystal shows good transmittance in the visible region which enables it to be a good material for optoelectronic applications. As observed in the spectrum, the pure LSM crystal was transparent in the region from 250 nm to 800 nm. The lower cut-off wavelength for pure LSM is found at 235 nm. The wide range of transparency suggests that the crystals are good candidates for nonlinear optical applications.

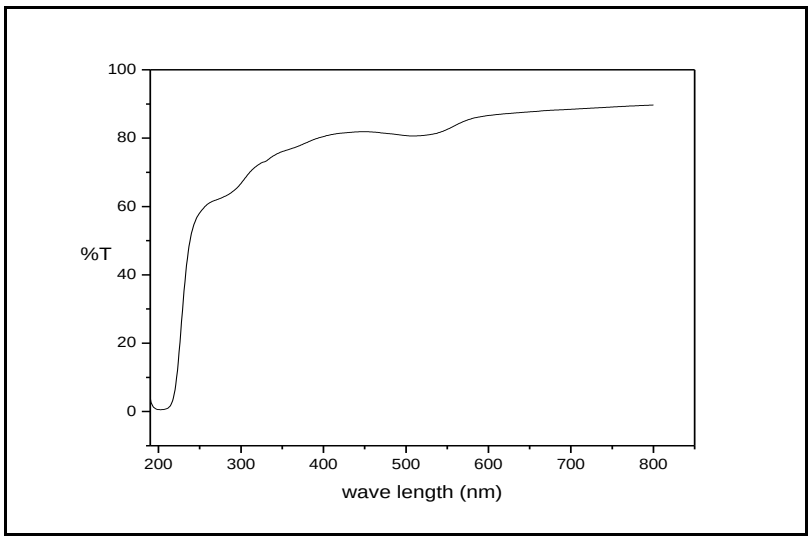

Fig. 9:UV–visible transmittance spectrum of LSM crystal

The optical absorption coefficient (α) was calculated using the following relation

$$\alpha = \frac{2.303}{d}\log\left(\frac{1}{T}\right) \qquad \textbf{(4)}$$

where T is the transmittance and d is the thickness of the crystal. As a direct band gap, the crystal under study has an absorption coefficient (α) obeying the following relation for high photon energies ($h\nu$).

$$\alpha = \frac{A(h\nu - E_g)^{\frac{1}{2}}}{h\nu} \qquad \textbf{(5)}$$

where E_g is the optical band gap of the crystal and A is a constant. Using the Tauc's relation, a graph (**Fig.10**) has been plotted between ($h\nu$) and ($\alpha\ h\nu$) ^{2} to estimate the direct band gap value, where α is absorption coefficient and $h\nu$ is the energy of the incident photon (E = $h\nu$). The energy gap (E_g) is determined by extrapolating the straight line portion of the curve to ($\alpha\ h\nu$)^2 = 0 From the plot, the band gap of LSM is found to be 5.28 eV which has close agreement with calculated value, 5.31 using the formula

$$E_g = \frac{1240}{\lambda}\ \text{eV} \qquad \textbf{(6)}$$

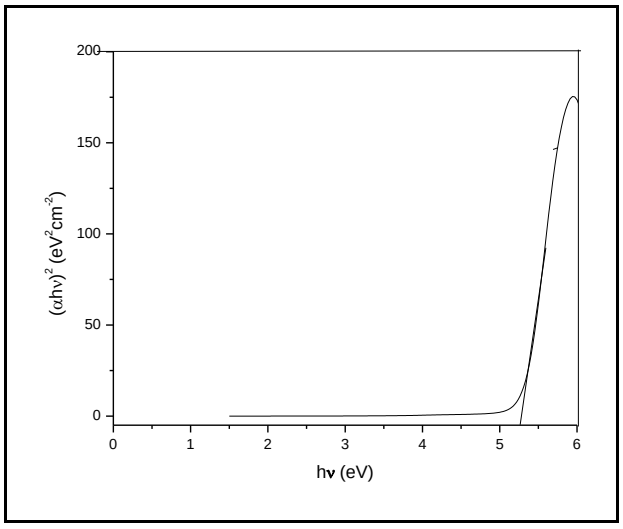

Fig. 10. **Tauc's plot of LSM crystal**

3.6. Scanning electron microscopy (SEM)

Figs.11 (a, b, c and d) show the SEM micrographs of grown LSM crystal surface with resolutions 100 μ m,40 μ m,20 μ m and 10 μ m respectively were recorded using SEM and EDAX techniques. The SEM photograph was taken using a scanning electron microscope with a magnification of 30 k to study the surface morphology. The surface features of grown crystals as shown in **Fig 11a** reveal the smooth surface of grown crystal with transparent nature. **Figs. 11(b, c and d)** show the different sizes of atoms confirming the presence of various components in the grown crystal.**Fig.12** shows EDAX spectrum of LSM crystal . The presence of elements S and O in different proportions are indicated by the respective peaks. The compositional analysis of LSM crystal from EDAX spectrum is shown in **Table 4.**

11.a) **11.b)**

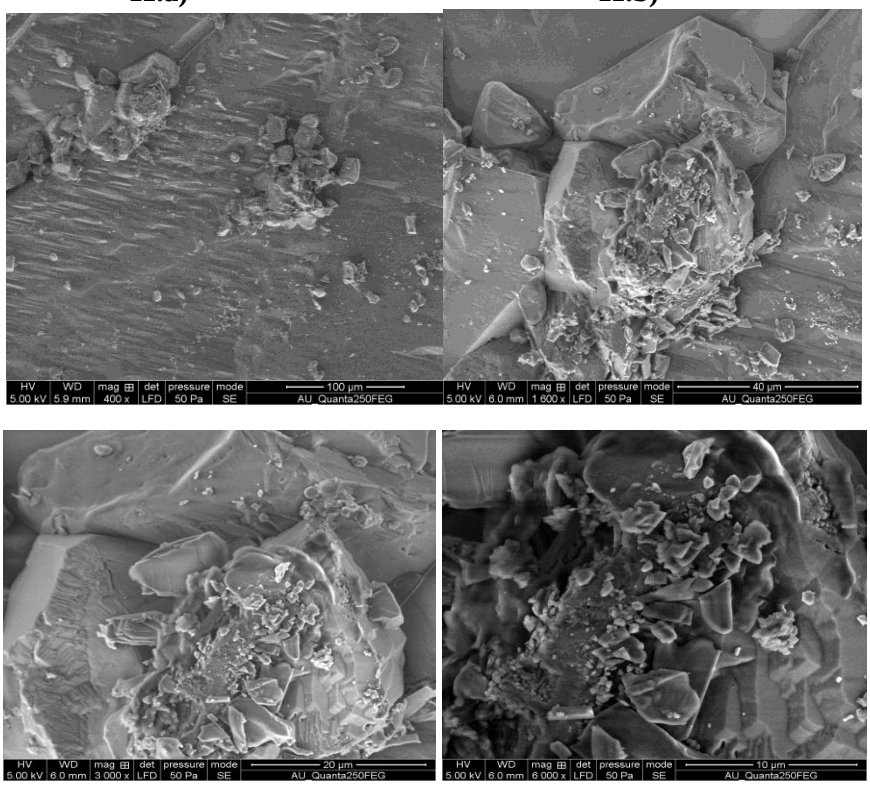

11.c) **11.d)**

Fig. 11. **SEM micrographs of LSM crystal**

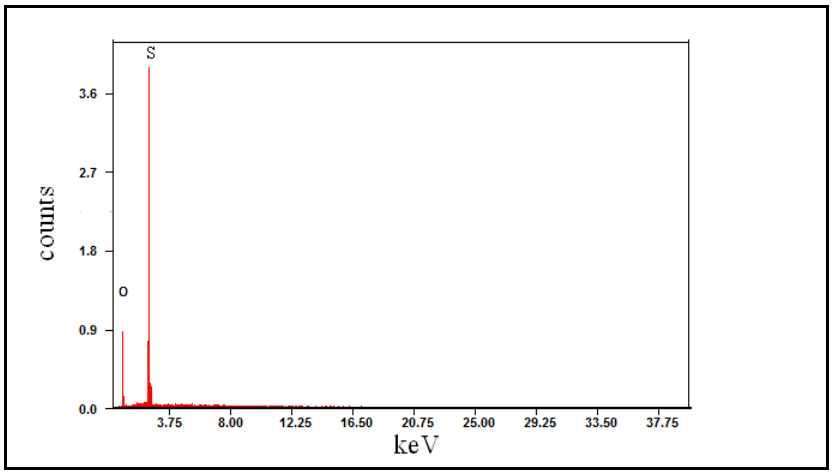

Fig. 12.EDAX analysis for LSM

Table 4 Compositional analysis of LSM crystal from EDAX spectrum.

Element	Wt%	Wt% (Calculated)
O	60.36	62.52
S	26.64	25.06
H	--	1.58
Li	--	10.85

3.7. NLO Study

The first and the most widely used technique for confirming the SHG from prospective second- order NLO material is the Kurtz and Perry powder technique [28]. Second harmonic generation efficiency of grown crystal LSM was estimated by Kurtz and Perry powder technique with the help of Nd:YAG laser beam of wavelength 1064nm.The crystalline LSM material was powdered to the particle size in the range 125-150 μm.The crystal was densely packed in a micro capillary tube. The first harmonic output of 1064nm from Nd:YAG laser was made to fall normally , passed through the pure LSM powder sample. The SHG behavior in these crystals was confirmed from the emission of intense green radiation (λ =532 nm) by the sample. The SHG efficiency of LSM was found to be less than that of KDP crystal by measuring the output voltage of the signal and comparing with that (36 mV) of KDP.

Conclusion

Good optical quality LSM crystals were grown using isothermal slow evaporation method. The solubility of LSM crystal is observed to be decreasing with increase in temperature (negative solubility). The reflection planes were identified using powder crystal X-ray diffraction technique. The functional groups present in the grown crystals have been confirmed by FTIR spectral analysis. The transparent range and the optical band gap of the crystal were measured using UV-vis-NIR spectrum. The microstructure of LSM crystal was analyzed using SEM photograph. The various elements present in the crystal were identified using EDAX analysis. TG-DTA studies reveal that the crystal LSM is thermally stable up to 156 ^{o}C. Vickers microhardness value was calculated in order to understand the mechanical strength of the grown crystal and the values of yield strength and stiffness constant were determined. The NLO efficiency of LSM sample is found to be slightly less than that of KDP. Therefore it is concluded that the inorganic LSM is a promising NLO material with enhanced SHG efficiency.

Acknowledgment

The author is grateful to the management of National Engineering College, Kovilpatti, for the encouragement given to carry out the research work. Research supports given by Aditanar College of Arts and Science, Tiruchendur, STIC, Cochin University, Alagappa University, Karaikudi and St.Joseph's college, Trichy, IISC, Bangalore are gratefully acknowledged.

References

1. V.G. Dmitriev, Gurzadyan, G. Gagik, Nikogosyan, N. David, Handbook of Nonlinear Optical Crystals, Springer, Berlin, Heidelberg, New York, Barcelona, Hong Kong, London, Milan, Paris, Singapore, Tokyo, 1999.
2. R.R. Levitskii, I.R. Zachek, A.S. Vdovych, S.I. Sorokov, Condens. Matter Phys. 12 (2009) 75–119.
3. B.D. Boyan, Z. Schwartz, Nat. Rev. Rheumatol. 7 (2011) 8–9.
4. D. Jugovic´ , D. Uskokovic´ , J. Power Sources 190 (2009) 538–544.
5. M.E. Hagerman, K.R. Poeppelmeier, Chem. Mater. 7 (1995) 602–621.
6. E.M. Brody, H.Z. Cummins, Phys. Rev. Lett. 21 (1968) 1263–1266.
7. A. Clearfield, D.S. Thakur, Appl. Catal. A 26 (1986) 1–26.
8. H. Onoda, K. Tange, I. Tanaka, J. Mater. Sci. 43 (2008) 5483–5488.
9. Y.S. Liu, W.B. Jones, J.P. Chernoch, Appl. Phys. Lett. 29 (1976) 32–34.
10. M.B. Danailov, I.Y. Milev, Appl. Phys. Lett. 61 (1992) 746–748.
11. X.D. Yang, Z.Z. Xu, Y.X. Leng, H.H. Lu, L.H. Lin, Z.Q. Zhang, R.X. Li, W.Q. Zhang, D.J. Yin, B. Tang, Opt. Lett. 27 (2002) 1135–1137
12. M.H. Jiang, Q. Fang, Advanced Materials 11 (1999) 1147.
13. J. Zyss, D.S. Chemla, J.F. Nicoud, Journal of Chemical Physics 74 (1981) 4800.
14. J.Chandrasekaran, P.Ilayabarathi, P.Maadeswaran, P.Mohamed Kutty, S.Pari, Optics Communications 285 (2012) 2096.
15. K. Boopathi,P.Rajesh,P.Ramasamy,Journal of Crystal Growth 345 (2012) 6.
16. D. Shanthi, P. Selvarajan, K.K. HemaDurga, S. Lincy Mary Ponmani, Spectrochimica Acta Part A 110 (2013) 1–6
17. A.SivaDhas, P.Selvarajan, T.H.Freeda, Materials and Manufacturing Processes, 24 (2009) 584– 589
18. A.Puhal Raj, C.Ramachandra Raja, Spectrochimica Acta Part A, 97 (2012) 83-87.
19. G. Rajadurai, A. Puhal Raj and S. Pari, Archives of Applied Science Research, 2013, 5 (3):247-253
20. W.Mott,Micro Indentation Hardness Testing, Butterworth's,London, 1956.,P. 206.
21. B.R. Lawn, E.R. Fuller, Journal of Material Science 9 (1975) 2016.
22. J.H.Westbrook,Report58-RL-2033of the G.E.Research laboratory USA (1958).
23. K. Sangwal, B. Surowska, Materials Research Innovations 7 (2003) 91.
24. E.M. Onitsch,Microscope 12(1950)95.
25. K.Sangwal, Crystal Research and Crystal Technology 44 (10)(2009) 1019–1037
26. C. Hays, E.G. Kendall, Metallurgy 6, 275 (1973).
27. Wooster W A 1953 Rep. Prog. Phys. **16** 62.
28. S.K.Kurtz,T. T.Perry,A powder technique for the evaluation of non linear optical materials ,j. Appl.Phys.39(1968)3798-3813.

*****